Title: Warmer spring temperatures in temperate deciduous forests advance the timing of tree growth but have little effect on annual woody productivity

Authors:

Cameron Dow[1,2] (Orcid ID : 0000-0002-8365-598X)

Albert Y. Kim[1,3] (Orcid ID : 0000-0001-7824-306X)

Loïc D'Orangeville[4,5] (Orcid ID : 0000-0001-7841-7082)

Erika B. Gonzalez-Akre[1] (Orcid ID : 0000-0001-8305-6672)

Ryan Helcoski[1]

Valentine Herrmann[1] (Orcid ID : 0000-0002-4519-481X)

Grant L. Harley[6] (Orcid ID : 0000-0003-1557-8465)

Justin T. Maxwell[7] (Orcid ID: 0000-0001-9195-3146)

Ian R. McGregor[1,8] (Orcid ID: 0000-0002-5763-021X)

William J. McShea[1]

Sean McMahon[9,11] (Orcid ID : 0000-0001-8302-6908)

Neil Pederson[4] (Orcid ID : 0000-0003-3830-263X)

Alan J. Tepley[1,10] (Orcid ID : 0000-0002-5701-9613)

Kristina J. Anderson-Teixeira[1,11]* (Orcid ID : 0000-0001-8461-9713)

Author Affiliations:

1. Conservation Ecology Center; Smithsonian Conservation Biology Institute; Front Royal, VA 22630, USA
2. Department of Forestry and Natural Resources, Purdue University, West Lafayette, Indiana, USA
3. Statistical & Data Sciences; Smith College; Northampton, MA 01063, USA
4. Harvard Forest, Petersham, MA 01366, USA
5. Faculty of Forestry and Environmental Management, University of New Brunswick, Fredericton, NB, E3B 5A3, Canada.
6. Department of Earth and Spatial Sciences, University of Idaho, ID 83844, USA
7. Department of Geography, Indiana University, Bloomington, IN 47405, USA

8. Center for Geospatial Analytics; North Carolina State University; Raleigh, NC 27607, USA
9. Smithsonian Environmental Research Center, Edgewater, MD, USA
10. Canadian Forest Service, Northern Forestry Centre, Edmonton, Alberta, Canada
11. Forest Global Earth Observatory; Smithsonian Tropical Research Institute; Panama, Republic of Panama

*corresponding author: teixeirak@si.edu; +1 540 635 6546

As the climate changes, warmer spring temperatures are causing earlier leaf-out[1–6] and commencement of net carbon dioxide (CO_2) sequestration[2,4] in temperate deciduous forests, resulting in a tendency towards increased growing season length[1,4,5,7–9] and annual CO_2 uptake[2,4,10–14]. However, less is known about how spring temperatures affect tree stem growth, which sequesters carbon (C) in wood that has a long residence time in the ecosystem[15,16]. Using dendrometer band measurements from 463 trees across two forests, we show that warmer spring temperatures shifted the woody growth of deciduous trees earlier but had no consistent effect on peak growing season length, maximum daily growth rates, or annual growth. The latter finding was confirmed on the centennial scale by 207 tree-ring chronologies from 108 forests across eastern North America, where annual growth was far more sensitive to temperatures during the peak growing season than in the spring. These findings imply that extra CO_2 uptake in years with warmer springs[10–12] is not allocated to long-lived woody biomass, where it could have a substantial and lasting impact on the forest C balance. Rather, contradicting current projections from global C cycle models[2,3,17,18], our empirical results imply that warming spring temperatures are unlikely to increase the woody productivity or strengthen the CO_2 sink of temperate deciduous forests.

In recent decades, Earth's forests have sequestered ~20% of anthropogenic CO_2 emissions, thereby slowing the pace of atmospheric CO_2 accumulation and climate change[19,20]. A large portion of this CO_2 sink occurs in temperate deciduous forests, which sequester >300 Tg C yr^{-1} (>30% of the total forest C sink)[21]. The future behavior of this CO_2 sink will play an important yet uncertain role in influencing atmospheric CO_2 and climate change[20,22].

57 In temperate deciduous forests, spring warming generally lengthens the period over which
58 trees have photosynthetically active leaves[1,7–9] and that over which the ecosystem is a net CO_2
59 sink[2]. Current models assume that longer growing seasons lead to increasing annual net CO_2
60 uptake (i.e., net ecosystem exchange, *NEE*)[2,3,17]. However, recent experimental and observational
61 findings show that annual productivity can be limited by sink factors[17,23,24], and that positive
62 effects of warm springs are compensated by negative effects of accumulation of seasonal water
63 deficits[3]. These studies suggest that warmer spring temperatures may not have the expected
64 positive effect on forest CO_2 sequestration.

65 While responses of leaf phenology and seasonal *NEE* to warming spring temperatures have
66 been documented[1–4,7–9], little is known about how the longest-lived component of fixed C in
67 trees, the woody growth, is responding to warming spring temperatures. In fact, we are aware
68 of only one study that has documented stem-growth phenology of temperate deciduous forests
69 over multiple years[25]. The climate sensitivity of woody growth phenology in temperate
70 deciduous trees and its link to annual growth has never been studied *in-situ* (but see Ref.[24] for a
71 controlled sapling experiment).

72 Tree-ring records, which can be used to examine relationships of annual growth to temperature
73 but not to understand growth phenology, reveal that growth of temperate deciduous trees
74 tends to be most sensitive to temperature or potential evapotranspiration between late spring
75 and early summer[26,27], with some hints that warmer springs may have a modest positive effect
76 on growth[27]. Thus, tree-ring evidence does not necessarily align with the finding that warming
77 spring temperatures increase annual forest CO_2 uptake[2]. Characterizing phenological responses

of stem growth to warming spring temperatures is critical to bridging this conceptual disconnect and understanding how forest biomass growth is likely to change as the climate warms.

Here, we evaluate how early spring temperatures affect stem growth phenology, growth rates, and annual growth of temperate deciduous trees across eastern North America. To test whether warmer springs extend the period of stem growth, we used dendrometer band measurements on 463 trees across two mid-latitude forests. To test whether spring temperatures consistently increased annual growth, we analyzed 207 tree-ring chronologies from 108 forests.

Dendrometer band analysis

Using dendrometer band measurements taken throughout multiple growing seasons at the Smithsonian Conservation Biology Institute (SCBI; Virginia, USA; n = 123 trees from 2011-2020) and Harvard Forest (Massachusetts, USA; n = 340 trees from 1998-2003), we fit a logistic growth model[28] to determine the days of year (DOY) when 25, 50, and 75% annual growth were achieved (DOY_{25}, DOY_{50}, DOY_{75}), peak growing season length ($L_{pgs} = DOY_{75}\text{-}DOY_{25}$), the maximum daily growth rates (g_{max}) and the DOY on which it occurred ($DOY_{g_{max}}$), and total annual increment in diameter at breast height (ΔDBH; Fig. 1). This analysis was performed separately for ring- and diffuse-porous species, which differ in growth phenology[25]. These stem-growth milestones were compared to canopy foliage phenology (measured at ecosystem level via remote sensing).

(a)

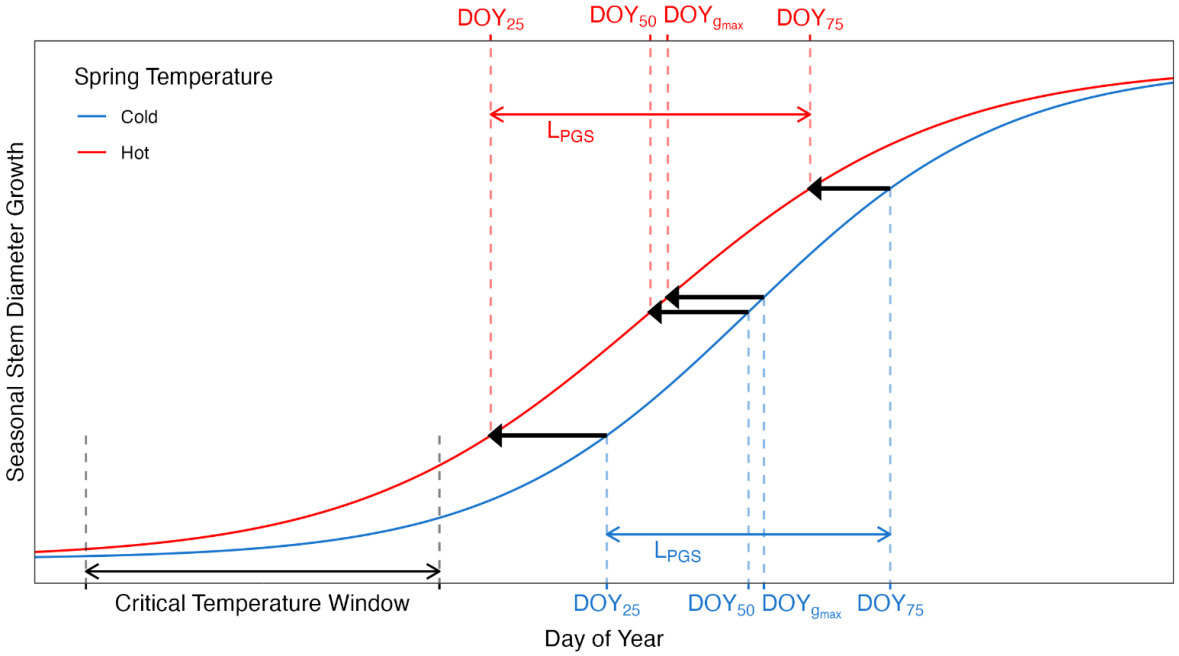

(b)

		Response to warmer spring T			
		SCBI		Harvard Forest	
Variable	Definition	RP	DP	RP	DP
Timing of growth					
DOY_{25}	day of year at which 25% of growth is achieved	↓	↓	↓	↓
DOY_{50}	day of year at which 50% of growth is achieved	↓	↓	↓	↓
DOY_{75}	day of year at which 75% of growth is achieved	↓	↓	↓	↓
$DOY_{g_{max}}$	day of year of max growth rate	↓	↓	↓	↓
L_{PGS}	peak growing season length ($DOY_{75} - DOY_{25}$)	↑	-	↓	↑
Daily growth rate					
g_{max}	maximum daily growth rate	-	-	↑	↓
Annual growth					
ΔDBH	annual growth	-	-	-	-
RWI	ring width index from tree-ring chronologies	mixed	mixed	-	mixed

Figure 1 | Summary of temperate deciduous tree growth responses to warmer spring temperatures. (a) Schematic illustrating parameters of interest and summarizing how each responds to warmer maximum temperatures during a 'critical temperature window', defined as the period with the strongest control over DOY_{25}; (b) Variable definitions and summary of responses to warmer spring temperatures at two temperate forests – Smithsonian Conservation Biology Institute (SCBI) and Harvard Forest – and for two groups of broadleaf deciduous species (RP=ring porous; DP=diffuse porous), where up and down arrows indicate significant increases and decreases, respectively, '-' indicates no significant correlation, and 'mixed' indicates a mix of significant and non-significant correlations, often in different directions.

Growth milestones for both canopy foliage phenology and stem growth occurred 6-10 days earlier, on average, at SCBI than at Harvard Forest (Fig. 2, Extended Data Table 2). Consistent with the results of Ref[25], ring-porous species began growing earlier, reaching the DOY_{25} benchmark earlier (by 31 days at SCBI and 32 at Harvard Forest), and their growth was spread over a longer growing season (average L_{PGS} 21 and 19 days longer at SCBI and Harvard Forest, respectively; Fig. 2, Extended Data Figure 2, Extended Data Table 2). Peak growing season length was similar across sites, with L_{PGS} being, on average, only two days longer at SCBI for ring-porous species and less than one day longer for diffuse-porous species (Extended Data Table 2).

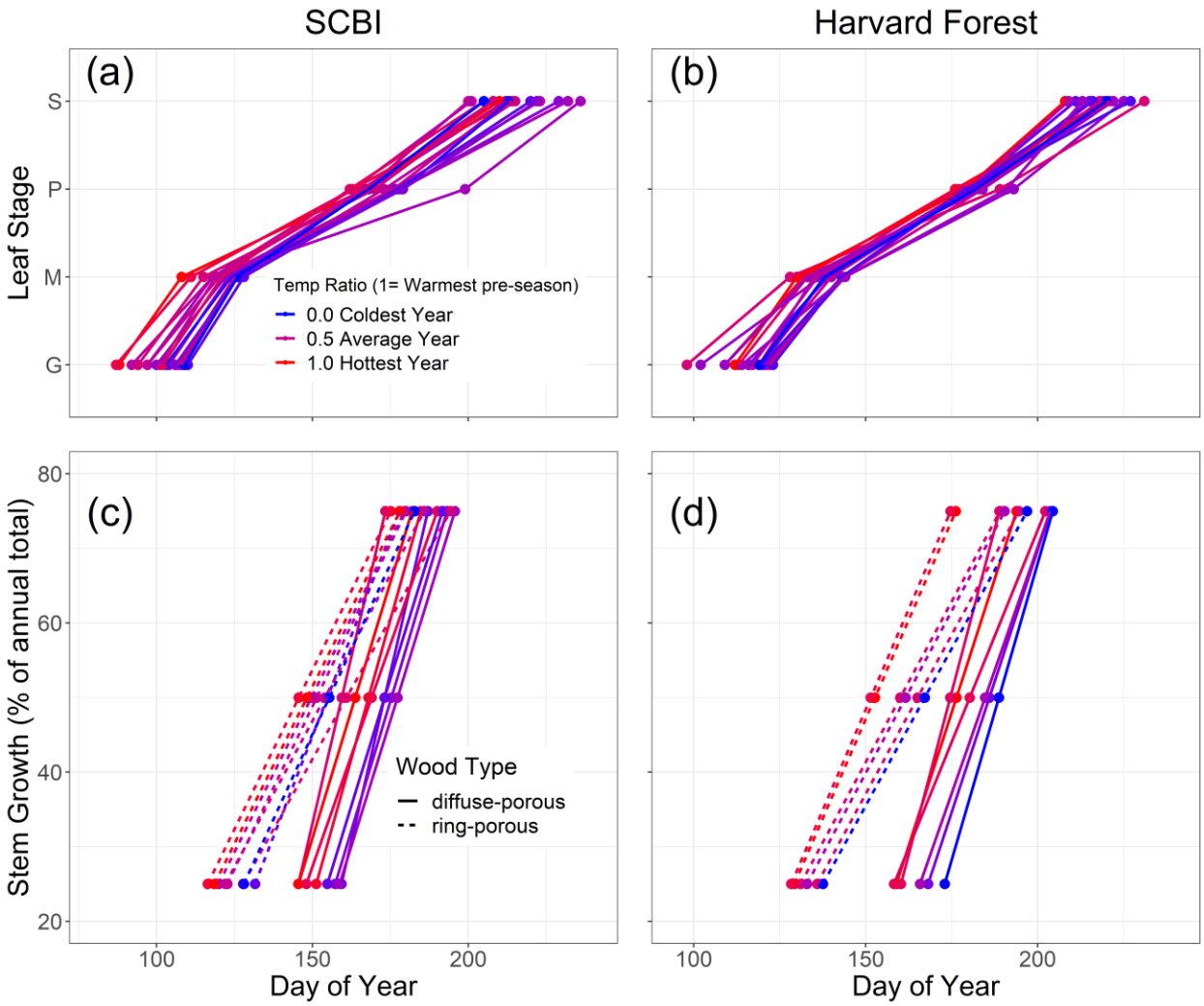

115

116 **Figure 2 | Foliage (a,b) and stem growth (c,d) phenology at the Smithsonian Conservation Biology**
117 **Institute (a,c) and Harvard Forest (b,d).** Panels (a-b) show ecosystem-level canopy foliage phenology
118 from 2001-2018, obtained from the MODIS Global Vegetation Phenology product (MCD12Q2.006), where
119 G = Greenup, M=Mid-greenup, P=peak, and S=Senescence (i.e., beginning of green-down). Panels (c-d)
120 show the dates at which stem growth milestones were achieved, on average, for sampled populations of
121 ring-porous and diffuse-porous trees at SCBI (2011-2020) and Harvard Forest (1998-2003). Mean
122 temperature was calculated for each wood-type/site combination over the respective critical T_{max}
123 window, then turned into a ratio and assigned a color on a gradient where the coldest year in the sample
124 is blue and the warmest is red.

125

126 Both MODIS-derived canopy foliage phenology and dendrometer band measurements of stem

127 growth phenology generally shifted backwards as spring temperatures increased (Fig. 2,

128 Extended Data Figures 4-5). We found a consistent effect of temperature (T_{max} or T_{min})

129 throughout the spring, but the strongest effects on stem-growth phenology were found using
130 T_{max} during a critical temperatrue window (CTW). CTW was identified by measuring the
131 correlation between all combinations of weekly T_{max} and DOY_{25} from January 1 to mean DOY_{25}
132 for each xylem porosity-site combination (Extended Data Figure 3). The CTW was defined as
133 the week(s) which had the strongest correlation with DOY_{25}.

134 For ring- and diffuse- porous species at both sites, warmer T_{max} in the CTW resulted in earlier
135 achievement of phenological milestones. Consistent with findings from previous studies[30], leaf
136 phenological milestones advanced at both sites (Fig. 2a-b, Extended Data Table 2), with greenup
137 (DOY when EVI2 first crossed 15% of the segment EVI2 amplitude) advancing 4.5 days/°C at
138 SCBI (p=0.001) and 2.4 days/ °C at Harvard Forest (p=0.1). Similarly, at both sites, the stem
139 growth milestones DOY_{25}, DOY_{50}, DOY_{75}, and $DOY_{g_{max}}$ all decreased with mean T_{max} during the
140 critical temperature window (Figs. 1, 2c-d; Extended Data Figures 4-5). Specifically, DOY_{25},
141 DOY_{50}, and DOY_{75} advanced 1.1-1.9 days/ °C for ring-porous species and 3.5-3.6 days/ °C for
142 diffuse-porous species at SCBI, and 2.8-7.2 days/ °C for ring-porous species and 6.6-7.9 days/ °C
143 for diffuse-porous species at Harvard Forest (Extended Data Table 2).

144 Whereas the length of time between canopy greenup and senescence (*i.e.,* the day when
145 greenness dropped below 90% of its peak) increased in years with warmer temperatures during
146 the critical temperature window compared to those with cooler temperatures (Fig. 2a-b), there
147 was no consistent lengthening of L_{PGS} (Fig. 1, Extended Data Figures 4-5).

148 In contrast to the pronounced effects of T_{max} on the timing of growth, its effects on g_{max} and
149 ΔDBH were weak and inconsistent (Figs. 1, Extended Data Figures 4-5). Specifically, g_{max},

which occurred very close to DOY_{50} (on $DOY_{g.max}$; Extended Data Table 2), displayed either no relationship to mean T_{max} during the critical temperature window (SCBI), or extremely small changes in opposite directions for ring- and diffuse- porous species (Harvard Forest). ΔDBH displayed no relationship with mean T_{max} during the critical temperature window (Extended Data Figure 4).

Tree-ring analysis

To understand how annual growth increments have responded to spring temperatures at the centennial scale, we analyzed tree-ring chronologies of 12 species at SCBI[27] and 4 species at Harvard Forest (Extended Data Table 1), along with an additional 191 chronologies from 106 sites (Fig. 3; Extended Data Figure 1; Extended Data Table 3)[26]. In total, our analysis included 207 chronologies representing 24 broadleaf species at 108 sites distributed from Alabama (Lat = 34.35) to Michigan (Lat = 45.56) and spanning a 15 °C range in April T_{max}. Across all chronologies, the standardized ring-width index (RWI) was significantly (at $p \leq 0.05$) positively correlated with April T_{max} for only 2% of chronologies: 1 of 142 ring-porous and 4 of 66 diffuse-porous species-site combinations (Extended Data Table 3). In contrast, RWI was frequently negatively correlated with T_{max} during peak growing season months (May-August), with significant correlations for 52% (May: 45/141, Jun: 107/141, Jul: 91/141, Aug: 53/141) and 46% (May: 10/66, Jun: 52/66, Jul: 36/66, Aug: 23/66) of species-site-month combinations for ring-porous and diffuse-porous species, respectively. T_{min} generally exibited weaker relationships to annual growth than T_{max}, with few significant correlations between spring T_{min} and RWI (Extended Data Figure 6).

171 To test whether the negative effect of summer temperatures might offset an enhancement of
172 growth by warmer spring temperatures, we tested for the joint effects of April and June-July
173 T_{max} on RWI. Results were qualitatively similar to the univariate correlations (Fig. 3), with
174 significant (at p = 0.05) positive correlations to April T_{max} for only 4% of chronologies and
175 significant negative correlations with June-July T_{max} for 77% of chronologies, supporting that
176 summer temperatures were the more important driver of annual stem growth (Extended Data
177 Table 3).

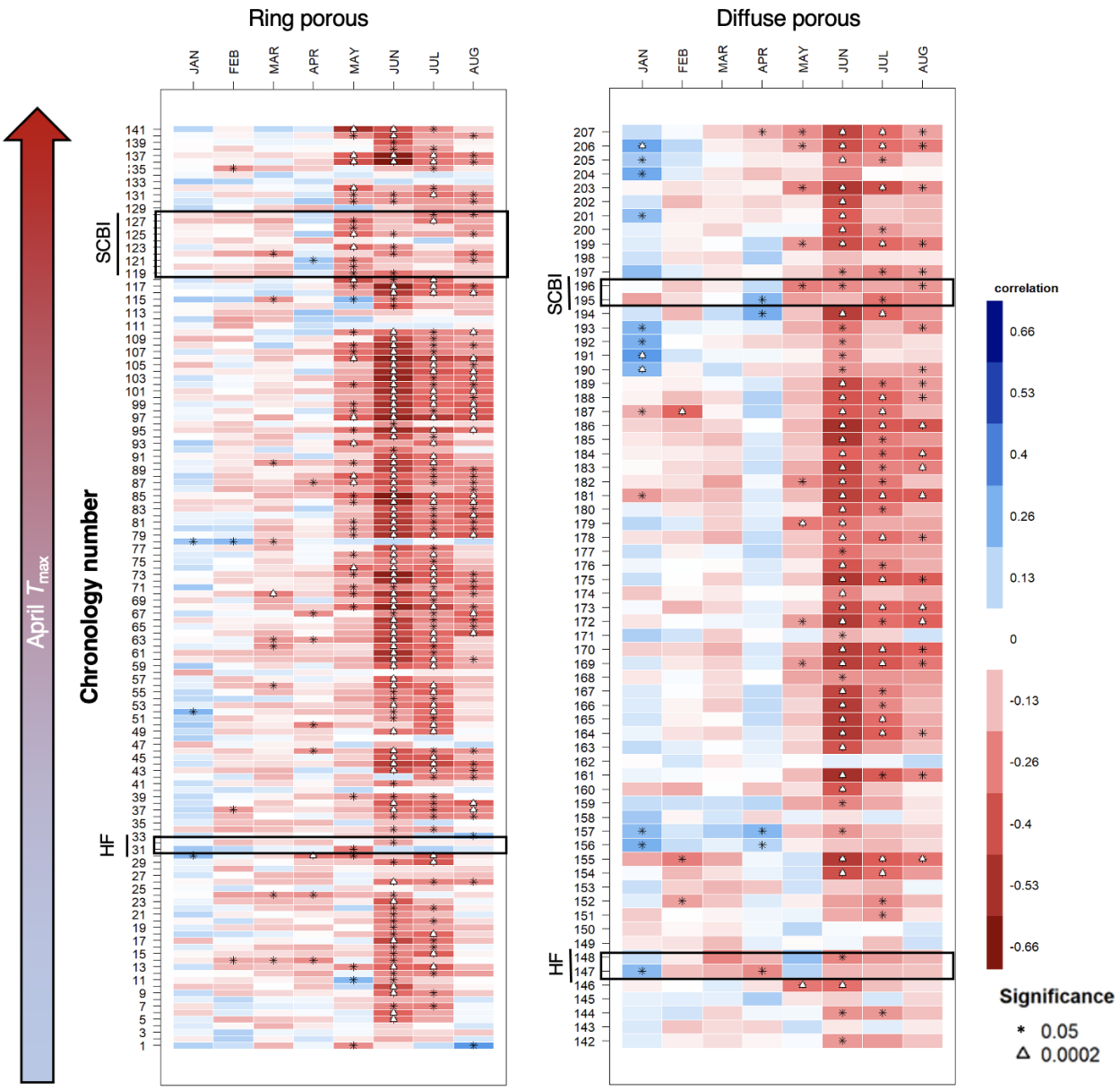

178

179 **Figure 3 | Sensitivity of annual growth, as derived from tree-rings, to monthly mean maximum**
180 **temperatures (T_{max}), for 207 chronologies from 108 sites across eastern North America** (Extended Data
181 Figure 1). Colors indicate the correlation between monthly T_{max} and a dimensionless ring width index
182 (RWI) derived from the multiple trees that form each chronology and emphasizing interannual variability
183 associated with climate. Chronologies are grouped by xylem porosity and ordered by mean April T_{max}.
184 Plots are annotated to highlight records from our two focal sites, the Smithsonian Conservation Biology
185 Institute (SCBI) and Harvard Forest (HF) (Extended Data Table 1). Species analyzed and numbers of
186 significant correlations to T_{max} are summarized in Extended Data Table 3, and chronology details are
187 given in SI Table 1.

Discussion

Together, our results demonstrate that warmer spring temperatures in the temperate deciduous forests of eastern North America advance the phenology of tree stem growth but have little effect on annual woody productivity (Figs. 1- 3). The observed phenological advance in the start of stem growth under warmer springs parallels phenological advances observed for canopy foliage (Fig. 2a-b)[2,4,5] and *NEE*[2,4]. However, inconsistent with the concept that an earlier start to growth would increase annual woody productivity, we demonstrate that warmer springs hasten the cessation of stem expansion and thereby have negligible effect on total annual growth for most species and locations (Fig. 3). Our observations suggest that the cessation of rapid stem expansion, which occurs mid-summer near the time of peak canopy greenness (Extended Data Figure 2)[4], is likely driven by cues other than photosynthate limitation, such as daylength or sink limitation, which also play an important role in autumn leaf senescence[17,23,31]. Our tree-ring analysis (Fig. 3) demonstrates that the primary effect of warming temperatures on annual tree growth is not an augmentation through an earlier start to growth, but rather a reduction associated to drought stress during the peak growing season[26]. Warm springs may also amplify summer drought stress in some times and places, effectively canceling out any positive effects of an extended growing period[3,32]; however, spring temperatures and summer Standardized Precipitation Evapotranspiration Index[33] were uncorrelated within our dendrometer band analysis, implying that the effects of warm spring temperatures on growth phenology elucidated here (Fig. 1) were not attributable to summer drought.

Our finding that interannual variation in woody growth is more strongly linked to conditions during the peak growing season than to growing season length aligns with parallel findings for *NEE*[13,14]. However, there is also a disconnect with findings that *NEE* is at least modestly greater in years with warm springs[2] or long growing seasons[4,13,14]. Warming advances spring phenology and may advance or delay autumn senescence depending on timing of warming and water availability[12,34,35], with delays more common across eastern North America,[2–4] implying that warming temperatures are lengthening the period from peak stem growth to the cessation of CO_2 uptake by the ecosystem. We show that the extra C fixation in years with warm springs does not substantially augment woody growth, but it remains unclear how it is allocated within the ecosystem. There are two main possibilities, which hold contrasting implications for the response of forest C balance to rising spring temperatures.

One possibility is that extra photosynthate in years with warm springs may be allocated to woody growth without affecting diameter growth in the current year. It is theoretically possible that extra C is allocated to cell wall thickening, a process that lags behind stem expansion[36], or to a thicker layer of higher-density latewood, resulting in formation of more C-dense wood in years with warm springs. However, existing evidence indicates that warm springs have a neutral or negative effect on latewood width[37–39], which is more strongly controlled by summer drought stress[37,38], suggesting that a positive effect of warm springs on the total C content of annual rings is unlikely. Extra C could also be saved within trees as non-structural carbohydrates and used towards growth the following year[40,41], potentially including an earlier start to growth[31]. Extension of our tree-ring analysis revealed weak correlation between April T_{max} and growth the following year (sig. pos. correlations for 5/142 RP and 3/66 DP species-site

230 combinations, Fig. Extended Data Figure 7), although predominantly positive (non-significant)
231 correlations in RP species suggests that this dynamic may weakly influence their annual
232 growth. Thus, warm springs are unlikely to provide substantial, sustained C sinks under
233 warming spring temperatures.

234 A second possibility is that any additional C fixed during years with warm springs may be
235 allocated to plant functions other than stem growth, including respiration, reproduction, and
236 production of foliage, roots[24], or root exudates. Much of this C would have a relatively short
237 residence time within the ecosystem, and C loss through fall or winter respiration may offset
238 gains from an earlier spring[3,42]. However, C allocated to nonstructural carbohydrates or
239 relatively short-lived plant tissues would typically remain in the ecosystem beyond the end of
240 the year[40], such that the long-term effect of warm springs on the forest C balance would not be
241 captured in analyses of interannual variation[2,13,14]. Studies within or including the temperate
242 deciduous biome that examined long-term trends in growing season length and ecosystem C
243 uptake[2,4,10,11] – as opposed to their interannual variation – showed increasing trends in both
244 variables, suggesting that the C not allocated to woody productivity within the current year has
245 a multi-year residence time within the ecosystem. However, given our finding that warm
246 springs do not significantly enhance woody productivity, this C is likely to have a relatively
247 short residence time within the ecosystem.

248 Thus, a distinction between interannual variation and directional change may be critical when
249 considering how directional climate change is likely to affect tree growth and ecosystem C
250 dynamics. As discussed above, temporal lags between C uptake and release imply that the full

effects of warm spring temperatures on forest woody productivity and C cycling are unlikely to be apparent in analyses of interannual variation (including this analysis)[43]. Moreover, acclimation of trees to warming temperatures[44] and, on longer time scales, species adaptations and shifts in community composition[45] are likely to alter the phenology of forest C cycling. If we look across spatial gradients where the latter have had time to play out, we see that warmer spring temperatures are associated with earlier leaf-out[6] and longer growing seasons, which in turn are are correlated with greater tree growth[46], woody productivity[47], and *NEE*[48]. Thus, warming spring temperatures are expected to increase the biophysical potential for annual tree growth, but that potential is not being realized on an interannual time frame.

As climate change accelerates and spring temperatures become increasingly warmer, growing seasons will start earlier; however, barring rapid acclimation of forests to the warming conditions, an earlier onset of growth in the spring is unlikely to provide the sustained increase in CO_2 sequestration and ensuant negative climate change feedback that is anticipated in most climate forecasting models[2,3,17,18]. Rather, the dominant effect of rising temperatures on forest woody productivity will be a negative effect of high summer temperatures, which constitutes a positive feedback to climate change.

Methods

Dendrometer band analysis

Dendrometer band measurements were collected at SCBI[49] and Harvard Forest[4,25], both part of the Forest Global Earth Observatory (ForestGEO)[50,51]. SCBI (38.8935° N, 78.1454° W; elevation

273–338 m.a.s.l.) is located in the Blue Ridge Mountains at the northern end of Shenandoah National Park, 5 km south of Front Royal, Virginia. The forest is secondary and mixed age, having established in the mid-19th century after conversion from agricultural fields[49]. Dominant canopy species within the 25.6 ha ForestGEO plot include tulip poplar (*Liriodendron tulipifera* L.), oaks (*Quercus spp.*), and hickories (*Carya spp.*)[27]. The climate is humid temperate, with 1950-2019 mean annual precipitation of 1018 mm and temperatures averaging 1° C in January and 24° C in July[46].

Harvard Forest (42.5388° N, 72.1755° W, 340-368 m.a.s.l.) is located near the central Massachusetts town of Petersham. The forest is secondary and mixed age, having re-established around the beginning of the 20th century following agricultural use and significant hurricane damage in 1938. Dominant species within the 35 ha ForestGEO plot are hemlock (*Tsuga canadensis* (L.) Carrière), oak (*Quercus spp.*) and red maple (*Acer rubrum* L.). The climate is temperate continental, with 1950-2019 mean annual precipitation of 1104 mm and temperatures averaging -5° C in January and 22° C in July[46].

Metal dendrometer bands were installed on 941 trees within the SCBI and Harvard Forest ForestGEO plots. Bands were placed on dominant species, including two diffuse- and two ring-porous species at SCBI and eight diffuse- and three ring-porous species at Harvard Forest (Extended Data Table 1). Bands were measured with a digital caliper approximately every 1-2 weeks within the growing season from 2011-2020 at SCBI and 1998-2003 at Harvard Forest. The number of bands measured at each site fluctuated slightly as trees were added or dropped from the census (e.g., because of tree mortality). Across years, the number of bands sampled

averaged 129 (range: 91-138) at SCBI and 717 (range: 700-755) at Harvard Forest. In total, our analysis included 2459 tree-years (Extended Data Table 1).

Measurements were timed to begin before the beginning of spring growth and to continue through the cessation of growth in the fall. At SCBI, the median start date was April 14, which was adjusted forward when early leaf-out of understory vegetation was observed, with the earliest start date being March 30 (in 2020). Measurements were continued through to fall leaf senescence, with the median end date being October 17 and the latest end date November 26 (2012). Timing of measurements at Harvard Forest were similar, with the median start date of April 23 and median end date of October 30. 1998 was an anomalous year where initial measurements were taken on January 5, but not taken again until April 15. The latest end date was November 11, 2002.

The raw dendrometer band data were manually inspected before analysis. We screened the data for three classes of errors. First, when a measurement was drastically different from previous and following measurements, it was assumed to be a human error and the datapoint was removed. Second, when measurements remained essentially unchanged for several readings, followed by a sudden jump then return to a normal growth pattern, this was assumed to be a case where the band was stuck on the tree bark and then released. In these cases, the full annual record for the tree was removed. Third, data points that deviated substantially from normal growth patterns, but for unknown causes, were removed. If a majority of the data points fell into this class within a tree-year, the entire year was removed from the analysis.

We fit a five-parameter logistic growth model[28] to dendrometer band data from each tree-year to define phenological dates and growth rates (Fig. 1). In particular, we model the observed diameter at breast height (DBH) on a given day of the year (DOY; *i.e.*, julian days) as:

$$DBH = L + \frac{K - L}{1 + 1/\theta \cdot exp[-r(DOY - DOY_{ip})/\theta)]^{\theta}}$$

Here, L and K are lower and upper asymptotes of the model, corresponding to DBH at the beginning and end of the year, respectively. DOY_{ip} is the day of year where the inflection point in growth rate occurs, r shapes the slope of the curve at the inflection point, and θ is a tuning parameter controlling the slope of the curve toward the upper asymptote. The DOY on which maximum growth occurs, $DOY_{g_{max}}$ (Fig. 1), occurs on DOY_{ip} when $\theta = 1$. The model was fit in R v4.0 using the functions developed in the *Rdendrom* package[28]. These functions take the time-series of manual dendrometer band measurements and return maximum-likelihood optimized values of the above five parameters that best predict DBH for each day of year. We then modeled DBH using these optimal parameter values in our logistic growth model and extracted the intra-annual growth variables of interest (Fig. 1).

After fitting the growth model, we removed tree-years with poor fits. Models were judged to be poorly fit if certain modeled growth characteristics fell outside of the logical range. Modeled fits for tree-years were removed under five conditions: (1) single day growth rates were ≥ 2 standard deviations away from the mean for each wood-type (SCBI = 2, Harvard Forest = 34); (2) DOY_{ip} was ≥ 2 standard deviations away from the mean for its xylem architecture group, year, and site (SCBI = 53, Harvard Forest = 106); (3) tree-years with small or negligible total

growth ($\Delta DBH \leq 0.02$ mm; SCBI = 0, Harvard Forest = 66); (4) model fit predicted total yearly growth to take longer than 365 days, indicating poor model fit (SCBI = 150, Harvard Forest = 199); (5) models with unexplained sharp spikes in growth rate (SCBI = 0, Harvard Forest = 3); and (6) poorly fit models that did not meet any of the above criteria (SCBI = 2, Harvard Forest = 0). At Harvard Forest the tag years removed through this method were proportional to the original sample size, indicating that no species or size class was disproportionately removed compared to others. At SCBI, a higher proportion of ring-porous trees were removed, the majority falling under condition 4.

Canopy foliage phenology data for the years 2001-2018 were extracted for SCBI and Harvard Forest from the MCD12Q2 V6 Land Cover Dynamics product (a.k.a. MODIS Global Vegetation Phenology product)[52] via Google Earth Engine. Extracted pixels were those containing the NEON tower at each site. Using daily MODIS 2-band Enhanced Vegetation Index data (EVI2) at a spatial resolution of 500m, the product yields the timing of phenometrics (vegetation phenology) over each year, including timing of greenup, midgreenup, and senescence as used in this study.

For the dendrometer band and leaf phenology analyses, climate data corresponding to the measurement periods were obtained from local weather stations at each focal site. For SCBI, weather data were obtained from a meteorological tower adjacent to the ForestGEO plot, via the ForestGEO Climate Data Portal v1.0 (https://forestgeo.github.io/Climate/)[53]. The R package *climpact* (see www.climpact-sci.org)[54] was used to plot temperatures for visual inspection and to identify readings that were >3 standard deviations away from yearly means, which were

352 labeled as outliers and removed from the dataset. Gaps in the SCBI meteorological tower data
353 were subsequently filled using temperature readings obtained from a National Center for
354 Environmental Information (NCEI) weather station located in Front Royal, Virginia
355 (https://www.ncdc.noaa.gov/cdo-web/datasets/GHCND/stations/GHCND:USC00443229/detail).
356 Daily temperature records for Harvard Forest, which had already been gap-filled based on
357 other local records, were obtained from the Harvard Forest weather station[55,56]. For each site, we
358 used records of daily maximum (T_{max}) and minimum temperatures (T_{min}).

359 The critical temperature window (CTW, Fig. 1), defined as the period over which T_{max} was
360 most strongly correlated with DOY_{25}, was determined using the R package *climwin*[57]. This
361 package tests the correlation between one or more predictor climate variable and a biological
362 outcome variable over all consecutive time windows within a specified time-frame. It does so
363 by reporting the correlation and $\Delta AICc$, the difference in Akaike Information Criterion corrected
364 for small sample size relative to a null model for each window. Here, we tested for correlation
365 between temperature predictor variables (T_{max}, T_{min}) and biological outcome variable DOY_{25}
366 over the time-frame from January 1 to the mean DOY_{25} for the species group (by xylem porosity)
367 and site (Extended Data Table 2). The time period yielding the lowest $\Delta AICc$ was selected as the
368 CTW. Because T_{max} proved to have a generally stronger influence over DOY_{25} and other growth
369 parameters, we focused on this variable in our ultimate model, as opposed to T_{min}. We defined
370 CTW for DOY_{25}, as opposed to other growth phenology parameters, because spring
371 temperatures should have the most direct influence on this variable.

To ensure that patterns were robust under an alternative definition of CTW, and to parallel the monthly time windows used in our tree-ring analysis (detailed below; Fig. 3, Extended Data Figure 6-7), we also ran analyses where we fixed the CTW to be the month of April. This was consistent with the periods identified by *climwin* for ring- and diffuse-porous species groups at both sites, all of which included all or part of April (Extended Data Table 2).

Correlation between the dendrometer band-derived growth parameters (DOY_{25}, DOY_{50}, DOY_{75}, $DOY_{g_{max}}$, L_{PGS}, g_{max}, and ΔDBH}, Fig. 1) and spring temperatures were assessed using a linear mixed model in a hierarchical Bayesian framework. Analyses were run for both T_{max} and T_{min}, with qualitatively similar results, but we present only results for T_{max}, which had overall stronger correlation with growth parameters. Mixed effects models were used to test the response of growth phenology variables to fixed effects of xylem porosity and mean T_{max} (or T_{min}) during the CTW, along with random effects of species and of individual tree. We ran separate models for each species group at each site, and for the response of all growth phenology variables to T_{max} (or T_{min}). This mixed-effect model was run within a hierarchical Bayesian framework and fit using the `rstanarm` R interface to the Stan programming language[58,59]. In all cases unless otherwise specified, all prior distributions are set to be the weakly informative defaults.

To rule out the possibility that observed patterns were strongly influenced by summer drought, we examined the relationship between spring tempreatures and summer Standardized Precipitation Evapotranspiration Index[33]. The latter was obtained from the ForestGEO Climate Data Portal v1.0 (https://forestgeo.github.io/Climate/)[53,60,61]. Linear models were run with 4-, 6-,

and 12-month SPEI values of June, July, and August vs April T_{max} to determine if warm spring temperatures lead to greater summer drought stress. No significant correlations were found (all p>0.05).

Tree-ring analysis

We analyzed tree-ring records for 108 sites, including our focal sites. All cores had been previously collected, cross-dated, and measured using standard collection and processing methodologies[62].

Dominant tree species were cored at both SCBI[27,49] and Harvard Forest[4,63,64] following sampling designs that covered a broad range of DBH. We analyzed records for the ring- and diffuse-porous species at each site (Extended Data Table 1), but excluded species with other xylem architectures (*Juglans nigra* L. at SCBI, *Tsuga canadensis* at Harvard Forest). We studied a total of 976 cores which included 12 species at SCBI and 4 species at Harvard Forest (Extended Data Table 1).

The tree-ring records from our focal sites were complemented with a much larger collection spanning 106 deciduous and mixed forest sites in Eastern North America[26,65]. Again, records were limited to broadleaf deciduous species with clearly defined xylem porosity (*i.e.*, excluding semi-ring porous).

For each species-site combination, we converted tree-ring records into the dimensionless RWI to emphasize interannual variability associated with climate.[66] A 2/3rds *n* spline was applied to each core using ARSTAN to produce standardized ring-width series; *n* is the number of years in

each series[66,67]. An adaptive power transformation, a process that also stabilises the variance over time[68], was used to minimize the influence of outliers in all series. Low series replication, often in the earliest portions of a chronology collection, can also inflate the variance of tree-ring records[69]. The 1/3rds spline method was chosen when replication in the inner portion of each chronology (ca. inner 30–50 yr of each record depending on full chronology length) was less than three trees. When replication was greater than n = 3 trees, we used the average correlation between raw ring-width series (rbar) method. The robust biweight mean chronology (RWI) for each species-site combination was calculated from the ring-width indices following variance stabilisation[67]. We defined chronology start year (Extended Data Table 1) as the year where subsample signal strength (SSS) passed a threshold of SSS = 0.8, or where ≥ 80% of the population signal was captured in the chronology.

For the analysis of correlation between RWI and climate variables, we obtained monthly T_{max} and T_{min} data for 1901-2019 from CRU v.4.04.[70] Correlations between monthly climate and RWI were assessed using 'dplR'[71] and 'bootRes'[72] in R v 4.0 (R Core Team, 2020), which correlated functions and bootstrapped confidence intervals for these relationships[73]. We analyzed these correlations for January through September of the current year (presented in Fig. 3, Extended Data Figure 6). To test for potential lag effects of spring temperatures on growth the following year, we also ran a version of the analysis extending back to include climate of every month of the previous year (Extended Data Figure 7). Correlations and significance levels for months April-August are given in SI Table 1.

We used a multivariate model to test for joint effects of April and summer T_{max} on RWI. We began by testing univariate correlations of T_{max} over three summer windows: June, June-July, and May-August. Having determined that, among these, June-July explained the most variation, we then analyzed the joint effects of April T_{max} and June-July T_{max} on RWI for each chronology independently using the base lm() function in R. Slopes and p-values for each chronology are given in SI Table 1.

Acknowledgements

We gratefully acknowledge all researchers who assisted with data collection in the field and laboratory, particularly Tsun Fung Au, Joshua Bregy, James Dickens, Karen Heeter, Anna Hennage, Daniel King, James McGee, Benjamin Lockwood, Jennifer McGarvey, Victoria Meakem, Josh Oliver, Jessica Shue, Karly Schmidt-Simard, Brandon Strange, Alyssa Terrell, Brynn Taylor, Michael Thornton, Senna Robeson, Matt Wenzel, and Luke Wylie. Thanks to David A. Orwig and members of the ForestGEO Ecosystesms & Climate Lab at SCBI for helpful feedback. The research was funded by ForestGEO (Smithsonian). Collection of tree-ring samples was funded by a USDA Agriculture and Food Research Initiative grant 2017-67013-26191 and from the Indiana University Vice Provost for Research Faculty Research Program.

Author Contributions

Cameron Dow and Kristina J. Anderson-Teixeira conceived the ideas and designed the study; Cameron Dow, Loïc D'Orangeville, Erika B. Gonzalez-Akre, Ryan Helcoski, Grant L. Harley,

Justin T. Maxwell, Ian R. McGregor, William McShea, Neil Pederson, Alan J. Tepley, and Kristina J. Anderson-Teixeira collected or oversaw collection of data; Cameron Dow, Albert Y. Kim, Valentine Herrmann, Justin T. Maxwell, Ian R. McGregor, Sean McMahon analyzed the data or provided analytical tools; Cameron Dow and Kristina J. Anderson-Teixeira led the writing of the manuscript. All authors contributed critically to the drafts and gave final approval for publication.

Additional Information

Supplementary Information is available for this paper.

Correspondence and requests for materials should be addressed to Kristina Anderson-Teixeira (teixeirak@si.edu).

References

1. Jeong, S.-J., Ho, C.-H., Gim, H.-J. & Brown, M. E. Phenology shifts at start vs. End of growing season in temperate vegetation over the Northern Hemisphere for the period 1982. *Global Change Biology* **17**, 2385–2399 (2011).

2. Keenan, T. F. *et al.* Net carbon uptake has increased through warming-induced changes in temperate forest phenology. *Nature Climate Change* **4**, 598–604 (2014).

3. Buermann, W. *et al.* Widespread seasonal compensation effects of spring warming on northern plant productivity. *Nature* **562**, 110–114 (2018).

4. Finzi, A. C. *et al.* Carbon budget of the Harvard Forest Long-Term Ecological Research site: Pattern, process, and response to global change. *Ecological Monographs* **90**, e01423 (2020).

5. Stuble, K. L., Bennion, L. D. & Kuebbing, S. E. Plant phenological responses to experimental warmingA synthesis. *Global Change Biology* **27**, 4110–4124 (2021).

6. Delgado, M. del M. *et al.* Differences in spatial versus temporal reaction norms for spring and autumn phenological events. *Proceedings of the National Academy of Sciences* 202002713 (2020) doi:10.1073/pnas.2002713117.

7. Menzel, A. & Fabian, P. Growing season extended in Europe. *Nature* **397**, 659–659 (1999).

8. Menzel, A. *et al.* European phenological response to climate change matches the warming pattern. *Global Change Biology* **12**, 1969–1976 (2006).

9. Ibáñez, I. *et al.* Forecasting phenology under global warming. *Philosophical Transactions of the Royal Society B: Biological Sciences* **365**, 3247–3260 (2010).

10. Keeling, C. D., Chin, J. F. S. & Whorf, T. P. Increased activity of northern vegetation inferred from atmospheric CO 2 measurements. *Nature* **382**, 146–149 (1996).

11. Dragoni, D. *et al.* Evidence of increased net ecosystem productivity associated with a longer vegetated season in a deciduous forest in south-central Indiana, USA. *Global Change Biology* **17**, 886–897 (2011).

12. Crabbe, R. A. *et al.* Extreme warm temperatures alter forest phenology and productivity in Europe. *Science of The Total Environment* **563–564**, 486–495 (2016).

13. Zhou, S. *et al.* Explaining inter-annual variability of gross primary productivity from plant phenology and physiology. *Agricultural and Forest Meteorology* **226–227**, 246–256 (2016).

14. Fu, Z. *et al.* Maximum carbon uptake rate dominates the interannual variability of global net ecosystem exchange. *Global Change Biology* **25**, 3381–3394 (2019).

15. Xue, B.-L. *et al.* Global patterns of woody residence time and its influence on model simulation of aboveground biomass. *Global Biogeochemical Cycles* **31**, 821–835 (2017).

16. Russell, M. B. *et al.* Residence Times and Decay Rates of Downed Woody Debris Biomass/Carbon in Eastern US Forests. *Ecosystems* **17**, 765–777 (2014).

17. Zani, D., Crowther, T. W., Mo, L., Renner, S. S. & Zohner, C. M. Increased growing-season productivity drives earlier autumn leaf senescence in temperate trees. 7 (2020).

18. Ahlström, A., Schurgers, G., Arneth, A. & Smith, B. Robustness and uncertainty in terrestrial ecosystem carbon response to CMIP5 climate change projections. *Environmental Research Letters* **7**, 044008 (2012).

19. Pan, Y. *et al.* A Large and Persistent Carbon Sink in the World's Forests. *Science* **333**, 988–993 (2011).

20. Friedlingstein, P. *et al.* Global Carbon Budget 2020. *Earth System Science Data* **12**, 3269–3340 (2020).

21. Pugh, T. A. M. *et al.* Role of forest regrowth in global carbon sink dynamics. *Proceedings of the National Academy of Sciences* **116**, 4382–4387 (2019).

22. Arora, V. K. *et al.* Carbonconcentration and carbonclimate feedbacks in CMIP6 models and their comparison to CMIP5 models. *Biogeosciences* **17**, 4173–4222 (2020).

23. Keenan, T. F. & Richardson, A. D. The timing of autumn senescence is affected by the timing of spring phenology: Implications for predictive models. *Global Change Biology* **21**, 2634–2641 (2015).

24. Zohner, C. M., Renner, S. S., Sebald, V. & Crowther, T. W. How changes in spring and autumn phenology translate into growth-experimental evidence of asymmetric effects. *Journal of Ecology* **109**, 2717–2728 (2021).

25. D'Orangeville, L. *et al.* Peak radial growth of diffuse-porous species occurs during periods of lower water availability than for ring-porous and coniferous trees. *Tree Physiology* (2021) doi:10.1093/treephys/tpab101.

26. D'Orangeville, L. *et al.* Drought timing and local climate determine the sensitivity of eastern temperate forests to drought. *Global Change Biology* **24**, 2339–2351 (2018).

27. Helcoski, R. *et al.* Growing season moisture drives interannual variation in woody productivity of a temperate deciduous forest. *New Phytologist* **223**, 1204–1216 (2019).

28. McMahon, S. M. & Parker, G. G. A general model of intra-annual tree growth using dendrometer bands. *Ecology and Evolution* **5**, 243–254 (2015).

29. Parmesan, C. & Yohe, G. A globally coherent fingerprint of climate change impacts across natural systems. *Nature* **421**, 37–42 (2003).

30. Friedl, M. A. *et al.* A tale of two springs: Using recent climate anomalies to characterize the sensitivity of temperate forest phenology to climate change. *Environmental Research Letters* **9**, 054006 (2014).

31. Fu, Y. S. H. *et al.* Variation in leaf flushing date influences autumnal senescence and next year's flushing date in two temperate tree species. *Proceedings of the National Academy of Sciences* **111**, 7355–7360 (2014).

32. Zhang, J. *et al.* Drought limits wood production of Juniperus przewalskii even as growing seasons lengthens in a cold and arid environment. *CATENA* **196**, 104936 (2021).

33. Vicente-Serrano, S. M., Beguería, S. & López-Moreno, J. I. A Multiscalar Drought Index Sensitive to Global Warming: The Standardized Precipitation Evapotranspiration Index. *Journal of Climate* **23**, 1696–1718 (2010).

34. Zohner, C. M. & Renner, S. S. Ongoing seasonally uneven climate warming leads to earlier autumn growth cessation in deciduous trees. *Oecologia* **189**, 549–561 (2019).

35. Xie, Y., Wang, X., Wilson, A. M. & Silander, J. A. Predicting autumn phenology: How deciduous tree species respond to weather stressors. *Agricultural and Forest Meteorology* **250–251**, 127–137 (2018).

36. Cuny, H. E. *et al.* Woody biomass production lags stem-girth increase by over one month in coniferous forests. *Nature Plants* **1**, 15160 (2015).

37. Tardif, J. C. & Conciatori, F. Influence of climate on tree rings and vessel features in red oak and white oak growing near their northern distribution limit, southwestern Quebec, Canada. *Canadian Journal of Forest Research* **36**, 2317–2330 (2006).

38. Roibu, C.-C. *et al.* The Climatic Response of Tree Ring Width Components of Ash (Fraxinus excelsior L.) And Common Oak (Quercus robur L.) From Eastern Europe. *Forests* **11**, 600 (2020).

39. Kern, Z. *et al.* Multiple tree-ring proxies (earlywood width, latewood width and δ13C) from pedunculate oak (Quercus robur L.), Hungary. *Quaternary International* **293**, 257–267 (2013).

40. Trumbore, S., Gaudinski, J. B., Hanson, P. J. & Southon, J. R. Quantifying ecosystem-atmosphere carbon exchange with a 14C label. *Eos, Transactions American Geophysical Union* **83**, 265–268 (2002).

41. Richardson, A. D. *et al.* Seasonal dynamics and age of stemwood nonstructural carbohydrates in temperate forest trees. *New Phytologist* **197**, 850–861 (2013).

42. Oishi, A. C. *et al.* Warmer temperatures reduce net carbon uptake, but do not affect water use, in a mature southern Appalachian forest. *Agricultural and Forest Meteorology* **252**, 269–282 (2018).

43. Kannenberg, S. A. *et al.* Linking drought legacy effects across scales: From leaves to tree rings to ecosystems. *Global Change Biology* **25**, 2978–2992 (2019).

44. Gessler, A., Bottero, A., Marshall, J. & Arend, M. The way back: Recovery of trees from drought and its implication for acclimation. *The New phytologist* **228**, 1704–1709 (2020).

45. Fisichelli, N. A., Frelich, L. E. & Reich, P. B. Temperate tree expansion into adjacent boreal forest patches facilitated by warmer temperatures. *Ecography* **37**, 152–161 (2014).

46. Anderson-Teixeira, K. J. *et al.* Joint effects of climate, tree size, and year on annual tree growth derived from tree-ring records of ten globally distributed forests. *Global Change Biology* **n/a**, (2021).

47. Banbury Morgan, R. *et al.* Global patterns of forest autotrophic carbon fluxes. *Global Change Biology* gcb.15574 (2021) doi:10.1111/gcb.15574.

48. Churkina, G., Schimel, D., Braswell, B. H. & Xiao, X. Spatial analysis of growing season length control over net ecosystem exchange. *Global Change Biology* **11**, 1777–1787 (2005).

49. Bourg, N. A., McShea, W. J., Thompson, J. R., McGarvey, J. C. & Shen, X. Initial census, woody seedling, seed rain, and stand structure data for the SCBI SIGEO Large Forest Dynamics Plot: *Ecological Archives* E094-195. *Ecology* **94**, 2111–2112 (2013).

50. Anderson-Teixeira, K. J. *et al.* CTFS-ForestGEO : A worldwide network monitoring forests in an era of global change. *Global Change Biology* **21**, 528–549 (2015).

51. Davies, S. J. *et al.* ForestGEO: Understanding forest diversity and dynamics through a global observatory network. *Biological Conservation* **253**, 108907 (2021).

52. Friedl, M., Gray, J. & Sulla-Menashe, D. MCD12Q2 MODIS/Terra+Aqua Land Cover Dynamics Yearly L3 Global 500m SIN Grid V006. (2019) doi:10.5067/MODIS/MCD12Q2.006.

53. Anderson-Teixeira, K. *et al.* Forestgeo/Climate: Initial release. (2020) doi:10.5281/ZENODO.4041609.

54. Benestad, R. E., Hanssen-Bauer, I. & Chen, D. *Empirical-statistical downscaling*. (World Scientific Pub Co Inc, 2008).

55. Boose, E. & Gould, E. Shaler Meteorological Station at Harvard Forest 1964-2002. (2021) doi:10.6073/PASTA/213335F5DAA17222A738C105B9FA60C4.

56. Boose, E. Fisher Meteorological Station at Harvard Forest since 2001. (2021) doi:10.6073/PASTA/69E92642B512897032446CFE795CFFB8.

57. van de Pol, M. *et al.* Identifying the best climatic predictors in ecology and evolution. *Methods in Ecology and Evolution* **7**, 1246–1257 (2016).

58. Gabry, J. *et al.* Rstanarm: Bayesian Applied Regression Modeling via Stan. (2020).

59. Stan_Development_Team. Stan Modeling Language Users Guide and Reference Manual, 2.28. (2019).

60. Beguería, S., Vicente-Serrano, S. M., Reig, F. & Latorre, B. Standardized precipitation evapotranspiration index (SPEI) revisited: Parameter fitting, evapotranspiration models, tools, datasets and drought monitoring. *International Journal of Climatology* **34**, 3001–3023 (2014).

61. Vicente-Serrano, S. M., Beguería, S. & López-Moreno, J. I. A Multiscalar Drought Index Sensitive to Global Warming: The Standardized Precipitation Evapotranspiration Index. *Journal of Climate* **23**, 1696–1718 (2010).

62. Stokes, M. A. & Smiley, T. L. *An Introduction to Tree-ring Dating*. (University of Arizona Press, 1968).

63. Alexander, M. R. *et al.* The potential to strengthen temperature reconstructions in ecoregions with limited tree line using a multispecies approach. *Quaternary Research* **92**, 583–597 (2019).

64. Dye, A. *et al.* Comparing tree-ring and permanent plot estimates of aboveground net primary production in three eastern U.S. forests. *Ecosphere* **7**, e01454 (2016).

65. Maxwell, J. T. *et al.* Sampling density and date along with species selection influence spatial representation of tree-ring reconstructions. *Climate of the Past* **16**, 1901–1916 (2020).

66. *Methods of Dendrochronology: Applications in the Environmental Sciences*. (Springer Netherlands, 1990). doi:10.1007/978-94-015-7879-0.

67. Cook, E. R. A Time Series Analysis Approach to Tree Ring Standardization. vol. PhD (University of Arizona, 1985).

68. Cook, E. R. & Peters, K. Calculating unbiased tree-ring indices for the study of climatic and environmental change. *The Holocene* **7**, 361–370 (1997).

69. Jones, P. D., Osborn, T. J. & Briffa, K. R. Estimating sampling errors in large-scale temperature averages. *Journal of Climate* **10**, 2548–2568 (1997).

70. Harris, I., Osborn, T. J., Jones, P. & Lister, D. Version 4 of the CRU TS monthly high-resolution gridded multivariate climate dataset. *Scientific Data* **7**, (2020).

71. Bunn, A. G. A dendrochronology program library in R (dplR). *Dendrochronologia* **26**, 115–124 (2008).

72. Zang, C. & Biondi, F. Dendroclimatic calibration in R: The bootRes package for response and correlation function analysis. *Dendrochronologia* **31**, 68–74 (2013).

73. Biondi, F. & Waikul, K. DENDROCLIM2002 : A C++ program for statistical calibration of climate signals in tree-ring chronologies. *Computers & Geosciences* **30**, 303–311 (2004).